

The Effect of Spatial Correlation on the Performance of Uplink and Downlink Single-Carrier Massive MIMO Systems

Nader Beigiparast, *Student Member*, Gokhan M. Guvensen, *Member*,
and Ender Ayanoglu, *Fellow*

Abstract

We present the analysis of a single-carrier massive MIMO system for the frequency selective Gaussian multi-user channel, in both uplink and downlink directions. We develop expressions for the achievable sum-rate when there is spatial correlation among antennas at the base station. We show that although the Channel Matched Filter Precoder (CMFP) performs the best in a spatially uncorrelated downlink channel, in a spatially correlated channel, CMFP does not perform as expected. We suggest better precoding schemes which lead to a better achievable sum-rate. Considering the same groups of users and antennas, we develop a model for the uplink channel. Using two equalizer structures, we show the results of system performance in terms of achievable rate at the base station.

Keywords: Single-carrier transmission, massive MIMO, wireless communication, uplink and downlink channel, precoding, equalization.

N. Beigiparast and E. Ayanoglu are with the Center for Pervasive Communications and Computing, Dept. EECS, UC Irvine, Irvine, CA, USA, G. M. Guvensen is with the Dept. of EEE, METU, Ankara, Turkey.

This work was partially supported by NSF under Grant No. 1547155.

This paper was partially presented during IEEE VTC2018-Spring.

I. INTRODUCTION

The demands for high-rate wireless communications have been increasing in the past few decades [1]. Due to this fact, there is a great amount of research on the development of new and efficient schemes to obtain higher rates of information for an increasing number of wireless channel users. Massive Multiple-Input Multiple-Output (Massive MIMO) is one of the approaches to achieve a higher rate in a wireless system. As a corollary of increasing the number of transmitters at the base station, the transmit power can be designed to be significantly small, since interference decreases at the same rate of the desired signal power, leading to a power-efficient system [2]. Also, the channel vectors (or matrices) defined between transmitters and receivers become asymptotically orthogonal, allowing multiple users to use the same bandwidth without interfering with each other and achieving a high spectral efficiency in the system [3]. However, in order to be able to use this method in an efficient way, better understanding of air interfaces, employment of precoders or equalizers in time or frequency domain, the optimum modulation technique, and limitations due to hardware impairments are needed.

In most studies of massive MIMO, the base station is considered to have the perfect knowledge of the channel, since massive MIMO relies on spatial multiplexing which requires good channel knowledge for the base station [4]. The base station can estimate the channel response to an individual user using the pilots sent by the terminals in the uplink. This process is more challenging in the downlink. The base station can send out pilot waveforms and users' terminals will be able to estimate the channel responses and feed them back to the base station. This solution was popular in conventional MIMO systems such as Long Term Evolution (LTE), however, it is not feasible in massive MIMO operation in an environment with high mobility [4]. Although, operating in time-domain-multiplexing (TDD) mode and employing the reciprocity of the uplink and the downlink is a general solution for massive MIMO, on the other hand, frequency-devision-multiplexing (FDD) mode can be a possible solution in specific cases [4].

It is critical to choose a suitable modulation scheme to cope with the massive MIMO channel. Orthogonal Frequency Division Multiplexing (OFDM) is one of the well-known modulation methods which has been studied in literature, see, e.g., [5]. In a system with OFDM, discrete Fourier transform and its inverse are important tools to deal with the frequency selectivity of the channel in the air interface. Discrete Fourier transforms also make the allocation of time or frequency resources feasible. A massive MIMO channel with OFDM modulation is considered the main technology in the downlink transmission in LTE [6], since OFDM modulation can convert a frequency selective channel into multiple sets of flat fading channels

and the benefits of MIMO systems can be easily obtained.

As an alternative approach to OFDM, single-carrier (SC) modulation has been introduced and was first investigated in a massive MIMO channel in [1]. Single-carrier transmission conventionally employs adaptive equalization techniques, however, in [1], the modulation uses the precoding technique to transmit symbols over the channel. In using single-carrier transmission, the main question is defining the equalization (or precoding) technique in either time or frequency domain. Although the frequency domain equalization techniques are usually preferred over the time domain ones because of the smaller complexity, see, e.g., [7], cyclic prefix and discrete Fourier transform modules are non-separable parts of the equalization techniques in the frequency domain. At the cost of increased complexity, time domain equalizers can achieve reasonable performance without requiring cyclic prefix or any discrete Fourier transforms. It is noteworthy to mention that single-carrier modulation combined with frequency domain equalization is a technique similar to OFDM which was proposed to combat intersymbol interference (ISI) without the Peak-to-Average Power Ratio (PAPR) growth of OFDM [8].

The work in this paper is focused on single-carrier transmission for massive MIMO applications. This is motivated by a number of recent studies such as [1]. This work showed that a Channel Matched Filter Precoder (CMFP) is optimum for such systems in channels uncorrelated in space. However, unlike [1], we wish to determine the performance of such systems for correlated channels, such as in massive MIMO where the presence of correlation in the channel is expected to be high due to space limitations for the antenna elements. Also, we expand our studies to the uplink channel, where equalizers are deployed at the base station side. Using the equalizers in the uplink and precoders in the downlink, we investigate the performance of the massive MIMO channel under the influence of correlation patterns. We would like to emphasize that unlike a conventional channel matched filter, CMFP is placed at the transmitter side [1].

II. DOWNLINK CHANNEL

In the downlink model, a frequency-selective multi-user MIMO (MU-MIMO) channel with M base station antennas and K single-antenna users is considered. We model the channel between the m -th transmit antenna and the k -th user as a finite impulse response (FIR) filter with L taps. The taps model different delay components. The l -th tap can be written as $\sqrt{d_l[k]}h_l^*[m, k]$ where $d_l[k]$ and $h_l^*[m, k]$ correspond to the slow-varying and fast-varying components of the channel respectively, and where $h_l[m, k]$ has a complex Gaussian distribution with zero mean and unit variance $\mathcal{CN}(0, 1)$ [1]. When the antenna elements or delay components are not correlated, the entries of the matrix consisting of the fast-varying

components of the channel, $h_l^*[m, k]$, are independent and identically distributed (i.i.d.). Further, these entries are fixed while the T symbols are being transmitted. Define $\mathbf{y}[i] \triangleq [y_1[i], \dots, y_K[i]]^T \in \mathbb{C}^K$ and $\mathbf{x}[i] \triangleq [x_1[i], \dots, x_M[i]]^T \in \mathbb{C}^M$ as the vector of received signals at each user and the vector of transmitted signals from each antenna at the base station at time $i = 1, 2, \dots, T$, respectively. Assume that the noise vector $\mathbf{n}[i] \triangleq [n_1[i], \dots, n_K[i]]^T$ is additive white Gaussian noise (AWGN) consisting of i.i.d. components and complex Gaussian distribution. We assume that this distribution has zero mean and unit variance. The variable $s_k[i]$ is the information symbol to be transmitted to the k -th user at time i . The vector of information symbols is defined as $\mathbf{s}[i] \triangleq [s_1[i], \dots, s_K[i]]^T$. This vector is considered to have i.i.d. $\mathcal{CN}(0, 1)$ components. We also need to define $\mathbf{D}_l \triangleq \text{diag}\{d_l[1], \dots, d_l[K]\}$, and $\mathbf{H}_l \in \mathbb{C}^{M \times K}$. The $[m, k]$ -th element of \mathbf{H}_l is $h_l[m, k]$.

In this paper, we will model the channel whose antenna elements have spatial correlation. To this end, we introduce the matrix $\mathbf{A} \in \mathbb{C}^{M \times M}$, taking into account all M antenna elements at the base station. The effect of this matrix on the channel will be to modify the channel realization from \mathbf{H}_l to $\mathbf{A}^{1/2}\mathbf{H}_l$. A channel whose antenna elements are not spatially correlated will have $\mathbf{A} = \mathbf{I}_M$. In Section V, we will make use of two commonly used spatial correlation models from the literature. Both of these models will have symmetric \mathbf{A} matrices.

The received signal vector can be written as

$$\mathbf{y}[i] = \sum_{l=0}^{L-1} \hat{\mathbf{H}}_l^H \mathbf{x}[i-l] + \mathbf{n}[i], \quad (1)$$

where the channel state information matrix is defined as $\hat{\mathbf{H}}_l = \mathbf{A}^{1/2}\mathbf{H}_l\mathbf{D}_l^{1/2}$ and the channel power delay profile (PDP) for each user is normalized such that [1]

$$\sum_{l=0}^{L-1} d_l[k] = 1, \quad k = 1, \dots, K. \quad (2)$$

Also, $\mathbf{x}[i]$ is the transmitted signal vector and it depends on the precoder used in the channel.

A. Channel Matched Filter Precoder (CMFP)

In wireless communication, the precoding scheme has a significant role. By using precoding techniques, one can reduce the PAPR and increase the signal-to-noise ratio (SNR) at the receiver [1]. The CMFP response matrix is the Hermitian of the channel state information matrix. Therefore, the transmit symbol vector can be written as

$$\mathbf{x}[i] = \sqrt{\frac{\rho_f}{MK}} \sum_{l=0}^{L-1} \hat{\mathbf{H}}_l^H \mathbf{s}[i+l], \quad (3)$$

in which $\rho_f \triangleq \mathbb{E}[\|\mathbf{x}[i]\|^2]$ is the total average power transmitted by the base station antennas. We define the super channel matrix as the multiplication of the precoder matrix and the channel information matrix $\mathbf{F}_{(l,l')} = \hat{\mathbf{H}}_l^H \hat{\mathbf{H}}_{l'}$. Note that one can obtain $\mathbf{F}_{(l,l')}[q, q'] = \mathbf{e}_q^T \mathbf{F}_{(l,l')} \mathbf{e}_{q'}$, where \mathbf{e}_q is a vector with all its elements equal to 0 except the q -th one which is 1. Using the channel composite matrix and placing (3) in (1), we can rewrite the received signal of the k -th user at time i as separate terms of the desired signal and the effective noise in the form

$$y_k[i] = \underbrace{\sqrt{\frac{\rho_f}{MK}} \left(\sum_{l=0}^{L-1} \mathbb{E}\{\mathbf{F}_{(l,l)}[k, k]\} \right) s_k[i]}_{\text{Desired Signal Term}} + \underbrace{n'_k[i]}_{\text{Effective Noise Term}}. \quad (4)$$

By an inspection of (1), (3), and (4), the effective noise term can be calculated as

$$\begin{aligned} n'_k[i] = & \sqrt{\frac{\rho_f}{MK}} \sum_{l=0}^{L-1} \left(\mathbf{F}_{(l,l)}[k, k] - \mathbb{E}\{\mathbf{F}_{(l,l)}[k, k]\} \right) s_k[i] + \sqrt{\frac{\rho_f}{MK}} \sum_{\substack{b=1-L \\ b \neq 0}}^{L-1} \sum_{l=L_1}^{L_2} \mathbf{F}_{(l,l-b)}[k, k] s_k[i-b] \\ & + \sqrt{\frac{\rho_f}{MK}} \sum_{\substack{q=1 \\ q \neq k}}^K \sum_{b=1-L}^{L-1} \sum_{l=L_1}^{L_2} \mathbf{F}_{(l,l-b)}[k, q] s_q[i-b] + n_k[i]. \end{aligned} \quad (5)$$

In (5), we defined $L_1 \triangleq \max(b, 0)$ and $L_2 \triangleq \min(L-1+b, L-1)$. In (5), the first term can be identified as the additional interference (IF), the second term as the intersymbol interference (ISI), and the third term as multiuser interference (MUI). The final term is AWGN.

In (4), for the desired signal term, the average power is equal to [1]

$$S_k = \mathbb{E}_{s_k[i]} \left\{ \left| \sqrt{\frac{\rho_f}{MK}} \sum_{l=0}^{L-1} \mathbb{E}\{\mathbf{F}_{(l,l)}[k, k]\} s_k[i] \right|^2 \right\} = \frac{M\rho_f}{K}. \quad (6)$$

The correlation matrix and the average power of the desired signal are independent, meaning that the desired signal power is not affected by the spatial correlation among antennas at the base station. The power of $n'_k[i]$, the effective noise in (5), can be calculated as

$$\text{Var}(n'_k[i]) = \frac{\text{tr}(\mathbf{A}^2)}{M} \rho_f + 1. \quad (7)$$

In (7), $\text{tr}(\mathbf{A}^2)$ is the trace of the square of the correlation matrix. We will introduce Proposition 1 and Proposition 2 below. These two propositions illustrate how (4) can be used to calculate the average power of the desired signal in (6) and the effective noise power in (7). For a channel without spatial correlation, (7) becomes $\rho_f + 1$. Although the average power of the desired signal and the correlation matrix are independent, the effective noise power is affected by the correlation matrix.

We are now interested in characterizing $\text{tr}(\mathbf{A}^2)$ for the spatially correlated channel. When we consider

the correlated case, the entries on the main diagonal of \mathbf{A} remain the same as the spatially uncorrelated case. On the other hand, other elements have nonzero values when there is correlation and for the models in this work, these values are nonnegative. Therefore, for the spatially correlated channel, $\text{tr}(\mathbf{A}^2) > M$. For this reason, the effective noise power will increase because of channel correlation. On the other hand, this does not affect the desired signal's average power. The correlation pattern makes the user information rate decrease, but the capacity remains the same. This implies an increase in correlation results in increased difference between the information rate and the capacity.

Each user's information rate as given in [1] can be obtained by $R_k = \log_2 \left(1 + \frac{M^2 \rho_f}{K \text{tr}(\mathbf{A}^2) \rho_f + KM} \right)$. By considering the fact that each user's information rate is almost equal to the other users', we will have the sum-rate as

$$R_{\text{sum}}(\rho_f, M, K) = K \log_2 \left(1 + \frac{M \rho_f}{K \frac{\text{tr}(\mathbf{A}^2)}{M} \rho_f + K} \right). \quad (8)$$

Since the correlation has no effect on the average power of the desired signal, the cooperative sum-capacity is independent of the correlation pattern and it can be written as [1]

$$C_{\text{coop}}(\rho_f, M, K) \approx K \log_2 \left(1 + \frac{M \rho_f}{K} \right). \quad (9)$$

Equations (8) and (9) are the sum rate (information rate) and the upper bound for CMFP, respectively, that will be illustrated in Fig. 1 and Fig. 2 in the sequel. By observing the information rate and the sum-capacity, one can conclude that CMFP may not be a good choice when there is sufficiently significant spatial correlation among the base station antennas. When the channel does not have spatial correlation, the effect of AWGN becomes more pronounced over the effective noise power. As a result, in that case, CMFP appears as a good choice for a precoder. When ρ_f reaches larger values, the information rate begins to saturate until the effective noise power is dominated by the interference terms. Computation results in Section V will verify this effect. As correlation increases, saturation happens earlier and quicker. The effect of any correlation among base station antennas is stronger interference terms that have a bigger effect than AWGN.

Proposition 1: The average power of the signal using CMFP is given as in (6).

Proof: In order to obtain the average power of the desired signal, we need the following lemma.

Lemma 1: Let \mathbf{x} and \mathbf{y} be N -dimensional zero-mean circularly symmetric complex Gaussian vectors with the autocorrelation and cross-correlation matrices given as $\mathbf{R}_x \triangleq \mathbb{E}\{\mathbf{x}\mathbf{x}^H\}$, $\mathbf{R}_y \triangleq \mathbb{E}\{\mathbf{y}\mathbf{y}^H\}$, and

$\mathbf{R}_{\mathbf{y}\mathbf{x}} \triangleq \mathbb{E}\{\mathbf{y}\mathbf{x}^H\}$. Then, the following expectations can be expressed as

$$\mathbb{E}\{\mathbf{x}^H \mathbf{A} \mathbf{y}\} = \text{tr}(\mathbf{A} \mathbf{R}_{\mathbf{y}\mathbf{x}}) \quad (10)$$

$$\mathbb{E}\{|\mathbf{x}^H \mathbf{A} \mathbf{y}|^2\} = \text{tr}(\mathbf{A}^T \mathbf{R}_{\mathbf{x}} \mathbf{A} \mathbf{R}_{\mathbf{y}}) + \text{tr}(\mathbf{A} \mathbf{R}_{\mathbf{y}\mathbf{x}}) \text{tr}(\mathbf{A}^T \mathbf{R}_{\mathbf{x}\mathbf{y}}) \quad (11)$$

in which \mathbf{A} is a real-valued and symmetric $N \times N$ matrix. The proof of this lemma is omitted here due to lack of space.¹

Consider the average power of the desired signal in (4) as

$$\begin{aligned} S_k &= \frac{\rho_f}{MK} \mathbb{E}_{s_k[i]} \left\{ \left| \sum_{l=0}^{L-1} \mathbb{E}\{\mathbf{F}_{(l,l)}[k, k]\} s_k[i] \right|^2 \right\} \\ &= \frac{\rho_f}{MK} \mathbb{E}_{s_k[i]} \left\{ \sum_{l'=0}^{L-1} s_k^H[i] \mathbb{E}\{\mathbf{F}_{(l',l')}[k, k]\} \sum_{l=0}^{L-1} \mathbb{E}\{\mathbf{F}_{(l,l)}[k, k]\} s_k[i] \right\}. \end{aligned} \quad (12)$$

We claim that the first multiplier can be written as

$$\sum_{l'=0}^{L-1} s_k^H[i] \mathbb{E}\{\mathbf{F}_{(l',l')}[k, k]\} = \sum_{l'=0}^{L-1} s_k^H[i] \mathbb{E}\{\mathbf{e}_k^T \mathbf{D}_{l'}^{1/2} \mathbf{H}_{l'}^H \mathbf{A} \mathbf{H}_{l'} \mathbf{D}_{l'}^{1/2} \mathbf{e}_k\}. \quad (13)$$

Let's focus on the term $\mathbb{E}\{\mathbf{F}_{(l,l)}[k, k]\}$. If we expand this term, it will be

$$\mathbb{E}\{\mathbf{F}_{(l,l)}[k, k]\} = \mathbb{E}\{\mathbf{e}_k^T \mathbf{D}_l^{1/2} \mathbf{H}_l^H \mathbf{A} \mathbf{H}_l \mathbf{D}_l^{1/2} \mathbf{e}_k\}. \quad (14)$$

Note that using $\mathbf{D}_l^{1/2} \mathbf{e}_k = \sqrt{d_l[k]} \mathbf{e}_k$, we can rewrite the above equation as

$$\mathbb{E}\{\mathbf{F}_{(l,l)}[k, k]\} = \sqrt{d_l[k]} \mathbb{E}\{\mathbf{h}_l^H[k] \mathbf{A} \mathbf{h}_l[k]\} \sqrt{d_l[k]}, \quad (15)$$

where $\mathbf{h}_l[k] \triangleq \mathbf{H}_l \mathbf{e}_k$. Note that $\mathbb{E}\{\mathbf{h}_l[k]\} = \mathbb{E}\{\mathbf{h}_l^H[k]\} = 0$ and $\text{Cov}\{\mathbf{h}_l[k]\} = \text{Cov}\{\mathbf{h}_l^H[k]\} = \mathbf{I}_K$. By using Lemma 1, one can say $\mathbb{E}\{\mathbf{h}_l^H[k] \mathbf{A} \mathbf{h}_l[k]\} = \text{tr}(\mathbf{A})$ which is equal to M . Therefore

$$S_k = \frac{\rho_f}{MK} \mathbb{E}_{s_k[i]} \{ |s_k[i]|^2 \} \left(M \sum_{l=0}^{L-1} d_l[k] \right)^2 = \frac{M \rho_f}{K}. \quad (16)$$

Based on Lemma 1, a set of expectations necessary to calculate the noise power in (7) is provided in the Appendix.

Proposition 2: The effective noise power using CMFP is given as in (7).

Proof: By an inspection of (5), we notice that different terms are independent from each other. Therefore, by using the expectations (58) and (61), we can write the variance of the effective noise as

$$\text{Var}\{n'_k[i]\} = \frac{\rho_f}{MK} \text{Var} \left\{ \sum_{l=0}^{L-1} \left(\mathbf{F}_{(l,l)}[k, k] - \mathbb{E}\{\mathbf{F}_{(l,l)}[k, k]\} \right) s_k[i] \right\}$$

¹One can use the moment generating function to obtain (10).

$$\begin{aligned}
& + \frac{\rho_f}{MK} \text{Var} \left\{ \sum_{\substack{b=1-L \\ b \neq 0}}^{L-1} \sum_{l=L_1}^{L_2} \mathbf{F}_{(l,l-b)}[k, k] s_k[i-b] \right\} \\
& + \frac{\rho_f}{MK} \text{Var} \left\{ \sum_{\substack{q=1 \\ q \neq k}}^K \sum_{b=1-L}^{L-1} \sum_{l=L_1}^{L_2} \mathbf{F}_{(l,l-b)}[k, q] s_q[i-b] \right\} + 1. \tag{17}
\end{aligned}$$

Note that the means of IF, ISI, and MUI terms are zero. Considering the fact that $\text{Var}\{s_k[i]\} = 1$ and the information symbols are independent from all other terms, after carefully reindexing (17) and removing a number of redundant terms, we can rewrite the effective noise variance as

$$\begin{aligned}
\text{Var}\{n'_k[i]\} &= \frac{\rho_f}{MK} \sum_{q=1}^K \sum_{b=1}^{L-1} \sum_{l=b}^{L-1} \mathbb{E} \left\{ \mathbf{F}_{(l,l-b)}[q, k] \mathbf{F}_{(l-b,l)}[k, q] \right\} \\
&+ \frac{\rho_f}{MK} \sum_{q=1}^K \sum_{b=1}^{L-1} \sum_{l=b}^{L-1} \mathbb{E} \left\{ \mathbf{F}_{(l-b,l)}[q, k] \mathbf{F}_{(l,l-b)}[k, q] \right\} \\
&+ \frac{\rho_f}{MK} \sum_{q=1}^K \sum_{l=0}^{L-1} \mathbb{E} \left\{ \mathbf{F}_{(l,l)}[q, k] \mathbf{F}_{(l,l)}[k, q] \right\} - \frac{\rho_f}{MK} \sum_{l=0}^{L-1} \left[\mathbb{E} \left\{ \mathbf{F}_{(l,l)}[k, k] \right\} \right]^2 + 1. \tag{18}
\end{aligned}$$

Then, if we replace the expectations inside (18) with their corresponding expressions in (55)-(61) in the Appendix, the effective noise variance can be obtained as

$$\begin{aligned}
\text{Var}\{n'_k[i]\} &= \frac{\text{tr}(\mathbf{A}^2) \rho_f}{MK} \sum_{q=1}^K \sum_{b=1}^{L-1} \sum_{l=b}^{L-1} (d_{l-b}[q] d_l[k] + d_l[q] d_{l-b}[k]) \\
&+ \frac{\text{tr}(\mathbf{A}^2) \rho_f}{MK} \sum_{q=1}^K \sum_{l=0}^{L-1} d_l[k] d_l[q] + 1. \tag{19}
\end{aligned}$$

One can recognize that (19) can be expressed as

$$\text{Var}\{n'_k[i]\} = \frac{\text{tr}(\mathbf{A}^2) \rho_f}{MK} \left[\sum_{q=1}^K \left(\sum_{l_1=0}^{L-1} d_{l_1}[q] \right) \left(\sum_{l_2=0}^{L-1} d_{l_2}[k] \right) \right] + 1 \tag{20}$$

Then, by using (2), (20) can be simplified as (7).

B. Conventional Precoders

The Zero-Forcing Precoder (ZFP) and Regularized Zero-Forcing Precoder (RZFP) are two well-known precoders in the massive MIMO field of study, see, e.g., [2]. A common theme among the precoders we will discuss in this paper is the fact that they are defined in the frequency domain and are translated into the time domain. Computations indicated that precoders defined in the time domain, such as those in [9], do not perform as well as precoders in the frequency domain. The two precoders will be given as functions of the channel state matrix $\hat{\mathbf{H}}_l$ as the following

- ZFP: It forces the system to eliminate the interference and is given by

$$\mathbf{W}_\nu^{ZFP} = a_W^{ZFP} \hat{\mathbf{H}}_\nu (\hat{\mathbf{H}}_\nu^H \hat{\mathbf{H}}_\nu)^{-1}, \quad (21)$$

where $\hat{\mathbf{H}}_\nu = \sum_{l=0}^{L-1} e^{-j2\pi\nu l/L} \hat{\mathbf{H}}_l$ is the N -point ($N > L$) Fourier transform of the channel state matrix and a_W^{ZFP} is a normalization factor for this precoder.

- RZFP: This precoder maximizes the power of the desired signal compared to the power of the noise and interference at the receiver. It is given by

$$\mathbf{W}_\nu^{RZFP} = a_W^{RZFP} \hat{\mathbf{H}}_\nu (\hat{\mathbf{H}}_\nu^H \hat{\mathbf{H}}_\nu + \beta_W \mathbf{I}_K)^{-1}, \quad (22)$$

where a_W^{RZFP} is also a power normalization factor and $\beta_W \in \mathbb{R}^+$ is a system parameter which depends on the SNRs and the path losses of the users.

Using these new precoders, one can generate a new model for the transmit signal vector. Using a general notation of \mathbf{W}_ν to indicate the precoder model, the transmit signal vector can be obtained as

$$\mathbf{x}[f] = \sqrt{\rho_f} \mathbf{W}_\nu \mathbf{s}[f], \quad (23)$$

where $\mathbf{s}[f] = \sum_{i=0}^{T-1} e^{-j2\pi f i/T} \mathbf{s}[i]$ and $\mathbf{x}[f] = \sum_{i=0}^{T-1} e^{-j2\pi f i/T} \mathbf{x}[i]$ are the Fourier transforms of the information symbols vector and the transmit signal vector, respectively. Note that in the definition of the precoders, we already consider the normalization factor. Considering the inverse Fourier transform, the vector of the transmit signals can be obtained in the time domain as the following

$$\mathbf{x}[i] = \sqrt{\rho_f} \sum_{m=0}^{N-1} \mathbf{W}_m \mathbf{s}[i-m], \quad (24)$$

where $\mathbf{W}_m = \sum_{\nu=0}^{N-1} e^{j2\pi\nu m/N} \mathbf{W}_\nu$ is the inverse Fourier transform of the precoder matrix. Note that (24) represents the cyclic convolution and all the indices of equation defining the transmit signal are taken modulo N (where $N > L$). Considering that (1) still holds, the vector of the received signals at the users' site can be written as

$$\mathbf{y}[i] = \sqrt{\rho_f} \sum_{m=0}^{N-1} \sum_{l=0}^{L-1} \hat{\mathbf{H}}_l^H \mathbf{W}_m \mathbf{s}[i-l-m] + \mathbf{n}[i]. \quad (25)$$

By defining the new super channel matrix as $\mathbf{F}_{(l,m)} = \hat{\mathbf{H}}_l^H \mathbf{W}_m$ and considering the fact that (24) represents circular convolution, one can rewrite (25) as

$$\mathbf{y}[i] = \sqrt{\rho_f} \sum_{m=1-N}^0 \sum_{l=0}^{L-1} \mathbf{F}_{(l,m)} \mathbf{s}[i-l-m] + \mathbf{n}[i]. \quad (26)$$

By changing the variable $m+l$ to b and considering the fact that $\mathbf{s}[i] = \sum_{q=1}^K \mathbf{e}_q s_q[i]$, we can rewrite (26)

as

$$\mathbf{y}[i] = \sqrt{\rho_f} \sum_{q=1}^K \sum_{b=1-N}^{L-1} \sum_{l=L_1}^{L_3} \mathbf{F}_{(l,b-l)}[:, q] s_q[i-b] + \mathbf{n}[i] \quad (27)$$

where $\mathbf{F}_{(l,b-l)}[:, q]$ is a column vector and where we defined $L_3 \triangleq \min(N-1+b, L-1)$. Note that the desired signal at the k -th user and time i is given by

$$g_k[i] = \sqrt{\rho_f} \sum_{l=0}^{L-1} \mathbb{E}\{\mathbf{F}_{(l,-l)}[k, k]\} s_k[i]. \quad (28)$$

Using the equations of the desired and received signal, one can express the system model in terms of desired signal and effective noise of the channel as

$$y_k[i] = g_k[i] + n'_k[i], \quad (29)$$

where $n'_k[i]$ represents the effective noise and can be written as

$$\begin{aligned} n'_k[i] = & \sqrt{\rho_f} \sum_{l=0}^{L-1} \left(\mathbf{F}_{(l,-l)}[k, k] - \mathbb{E}\{\mathbf{F}_{(l,-l)}[k, k]\} \right) s_k[i] + \sqrt{\rho_f} \sum_{\substack{b=1-N \\ b \neq 0}}^{L-1} \sum_{l=L_1}^{L_3} \mathbf{F}_{(l,b-l)}[k, k] s_k[i-b] \\ & + \sqrt{\rho_f} \sum_{\substack{q=1 \\ q \neq k}}^K \sum_{b=1-N}^{L-1} \sum_{l=L_1}^{L_3} \mathbf{F}_{(l,b-l)}[k, q] s_q[i-b] + n_k[i], \end{aligned} \quad (30)$$

which again includes IF, ISI, MUI, and AWGN terms, respectively. The system model introduced in this section is used to run computations. Note that since the power of the AWGN is considered to be 1, one can define the capacity of the system as

$$C_{sum} = \sum_{k=1}^K \log_2 (1 + S_k), \quad (31)$$

where one can obtain the power of the desired signal for the k -th user as it was calculated in Section II-A by $S_k = \mathbb{E}_{s_k[i]} \{|g_k[i]|^2\}$. The achievable sum-rate of the system can be obtained as

$$R_{sum} = \sum_{k=1}^K \log_2 \left(1 + \frac{S_k}{\text{Var}(n'_k[i])} \right). \quad (32)$$

Equations (31) and (32) are the upper bound and the sum-rate (information rate) for the precoders, respectively. They will also apply to the case of equalizers for the uplink channel as will be discussed in the next section. These equations will be employed in Fig. 3 through Fig. 15.

III. UPLINK CHANNEL

Just like the downlink model, a frequency-selective multi-user MIMO (MU-MIMO) channel with M base station antennas and K single-antenna users is considered. Perfect knowledge of channel state infor-

mation is considered at the users' terminal in the uplink transmission. Since the correlation pattern is also considered in the uplink channel, the channel state information matrix can be modeled as $\hat{\mathbf{H}}_l = \mathbf{A}^{1/2} \mathbf{H}_l \mathbf{D}_l^{1/2}$. Considering the uplink, users are supposed to transmit $\sqrt{\rho_f} \mathbf{s}[i]$ through the channel (to be able to control the power of the transmit signal from users' terminal, $\sqrt{\rho_f}$ has been added to the signal). However, using equalizers in the frequency domain at the base station requires employment of cyclic prefix techniques. In this work, the conventional cyclic prefix technique, where the last T_c samples of a T -sample transmission block are added to the beginning of the block, is preferred over the zero-padding or the known symbol padding techniques due to its circular convolution property [10].

In the same manner as it was introduced earlier in Section II, one can obtain the capacity and the achievable sum-rate of the uplink channel with an equalizer using (31) and (32), respectively. Note that S_k is the power of the desired signal for the k -th user at the base station and $n'_k[i]$ is the effective noise of the system for the k -th user at the base station at time i considering the uplink channel.

A. Channel Matched Filter Equalizer (CMFE)

The cyclic prefix is designed in the way that the length of the added symbols are larger than the length of the channel (i.e., $T_c > L$). We can write the received signal vector before applying the proper equalizer as

$$\mathbf{r}[i] = \sum_{l=0}^{L-1} \hat{\mathbf{H}}_l \mathbf{x}[(i-l) \bmod T] + \mathbf{n}[i], \quad (33)$$

where $\mathbf{x}[i]$ denotes the transmitted signal vector and consists of the transmitted symbols (e.g., $\sqrt{\rho_f} \mathbf{s}[i]$) and the T_c added symbols as the cyclic prefix. In this section, the channel matched filter is considered as the *equalizer* in the system. For that reason we designate it as CMFE, as opposed to CMFP employed in the downlink channel. The following shows how CMFE will affect the unprocessed output signal of the channel.

$$\mathbf{y}[i] = \frac{1}{\sqrt{MK}} \sum_{l=0}^{L-1} \hat{\mathbf{H}}_l^H \mathbf{r}(i+l), \quad (34)$$

where $\mathbf{y}[i]$ is the vector of the received signal after the equalizer block. Substituting (33) in (34), one can obtain

$$\mathbf{y}[i] = \sqrt{\frac{\rho_f}{MK}} \sum_{l=0}^{L-1} \sum_{l'=0}^{L-1} \hat{\mathbf{H}}_l^H \hat{\mathbf{H}}_{l'} \mathbf{s}[(i-l'+l) \bmod T] + \frac{1}{\sqrt{MK}} \sum_{l=0}^{L-1} \hat{\mathbf{H}}_l^H \mathbf{n}[i+l]. \quad (35)$$

We can rewrite the received signal for each individual user at the base station as the following

$$y_k[i] = g_k[i] + n'_k[i], \quad (36)$$

where $g_k[i]$ is the desired signal of the k -th user at the base station and can be written as

$$g_k[i] = \sqrt{\frac{\rho_f}{MK}} \left(\sum_{l=0}^{L-1} \mathbf{F}_{(l,l)}[k, k] \right) s_k[i \bmod T], \quad (37)$$

where $\mathbf{F}_{(l,l')} = \hat{\mathbf{H}}_l^H \hat{\mathbf{H}}_{l'}$ is the super channel matrix. The second is the effective noise of the system and, similar to the downlink channel, it can be written as

$$\begin{aligned} n'_k[i] = & \sqrt{\frac{\rho_f}{MK}} \sum_{\substack{b=1-L \\ b \neq 0}}^{L-1} \sum_{l=L_1}^{L_2} \mathbf{F}_{(l,l-b)}[k, k] s_k[(i-b) \bmod T] \\ & + \sqrt{\frac{\rho_f}{MK}} \sum_{\substack{q=1 \\ q \neq k}}^K \sum_{b=1-L}^{L-1} \sum_{l=L_1}^{L_2} \mathbf{F}_{(l,l-b)}[k, q] s_q[(i-b) \bmod T] + \frac{1}{\sqrt{MK}} \sum_{l=0}^{L-1} \mathbf{e}_k^T \hat{\mathbf{H}}_l^H \mathbf{n}[i+l]. \end{aligned} \quad (38)$$

As it can be seen, the effective noise term in the uplink is very similar to that of the downlink, except the difference of using CMFE makes in AWGN noise and perfect knowledge of CSI eliminates the IF term.

In order to determine the power of effective noise in the uplink channel, we need to determine the power of AWGN affected by CMFE, which is as the following

$$\begin{aligned} \text{Var}(z_k[i]) &= \text{Var} \left(\frac{1}{\sqrt{MK}} \sum_{l=0}^{L-1} \mathbf{e}_k^T \hat{\mathbf{H}}_l^H \mathbf{n}[i+l] \right) = \frac{1}{MK} \mathbb{E} \left(\sum_{l=0}^{L-1} \mathbf{e}_k^T \hat{\mathbf{H}}_l^H \mathbf{n}[i+l] \sum_{l'=0}^{L-1} \mathbf{n}^T[i+l'] \hat{\mathbf{H}}_{l'} \mathbf{e}_k \right) \\ &= \frac{1}{MK} \mathbb{E} \left(\sum_{l=0}^{L-1} \sum_{l'=0}^{L-1} \mathbf{e}_k^T \hat{\mathbf{H}}_l^H \mathbf{n}[i+l] \mathbf{n}^T[i+l'] \hat{\mathbf{H}}_{l'} \mathbf{e}_k \right) \\ &= \frac{1}{MK} \mathbb{E}_{H_l} \left(\sum_{l=0}^{L-1} \sum_{l'=0}^{L-1} \mathbf{e}_k^T \hat{\mathbf{H}}_l^H \mathbb{E}_{n[i]} \left(\mathbf{n}[i+l] \mathbf{n}^T[i+l'] \right) \hat{\mathbf{H}}_{l'} \mathbf{e}_k \right). \end{aligned} \quad (39)$$

By the nature of AWGN, if $l \neq l'$, then $\mathbb{E}_{n[i]} (\mathbf{n}[i+l] \mathbf{n}^T[i+l']) = \mathbf{0}_{M \times M}$. It will be equal to \mathbf{I}_M if $l = l'$.

Keeping this in mind, we can rewrite the power of the AWGN affected by CMFE as

$$\begin{aligned} \text{Var}(z_k[i]) &= \text{Var} \left(\frac{1}{\sqrt{MK}} \sum_{l=0}^{L-1} \mathbf{e}_k^T \hat{\mathbf{H}}_l^H \mathbf{n}[i+l] \right) = \frac{1}{MK} \mathbb{E}_{H_l} \left(\sum_{l=0}^{L-1} \mathbf{e}_k^T \hat{\mathbf{H}}_l^H \hat{\mathbf{H}}_{l'} \mathbf{e}_k \right) \\ &= \frac{1}{MK} \mathbb{E}_{H_l} \left(\sum_{l=0}^{L-1} \mathbf{e}_k^T \mathbf{D}_l^{1/2} \mathbf{H}_l^H \mathbf{A} \mathbf{H}_l \mathbf{D}_l^{1/2} \mathbf{e}_k \right) = \frac{\text{tr}(\mathbf{A})}{MK}. \end{aligned} \quad (40)$$

Therefore, using the power of AWGN affected by CMFE in (40) and the power of interference terms calculated in [11] neglecting the IF term, one can obtain the power of the effective noise in the uplink channel as

$$\text{Var}(n'_k[i]) = \frac{\text{tr}(\mathbf{A}^2)}{M} \left(1 - \sum_{l=0}^{L-1} \frac{d_l^2[k]}{K} \right) \rho_f + \frac{\text{tr}(\mathbf{A})}{MK}, \quad (41)$$

where $\text{tr}(\mathbf{A}) = M$ for the correlation patterns we consider in this work.

Based on what is stated in [11], the power of the desired signal can be obtained as $\frac{\rho_f}{MK} (\text{tr}(\mathbf{A}^2) \sum_{l=0}^{L-1} d_l^2[k] +$

$\text{tr}^2(\mathbf{A})(\sum_{l=0}^{L-1} d_l[k])^2$). Using (3) and by considering the fact that each user's capacity information rate is almost equal to the other users', we will have the capacity sum-rate as

$$C_{sum} = K \log_2 \left(1 + \frac{\rho_f}{MK} \text{tr}(\mathbf{A}^2) \sum_{l=0}^{L-1} d_l^2[k] + \frac{\rho_f}{MK} \text{tr}^2(\mathbf{A}) \right). \quad (42)$$

Using (4), one can obtain the achievable sum-rate as

$$R_{sum} = K \log_2 \left(1 + \frac{\text{tr}(\mathbf{A}^2) \sum_{l=0}^{L-1} d_l^2[k] \rho_f + \text{tr}^2(\mathbf{A}) \rho_f}{\text{tr}(\mathbf{A}^2)(K - \sum_{l=0}^{L-1} d_l^2[k]) \rho_f + M} \right). \quad (43)$$

B. Conventional Equalizers

Clearly, CMFE is a special case of implementing equalizers in the system. Using the general notation of \mathbf{Q}_ν to denote the equalizer equation in the frequency domain, one can obtain the received signal as

$$\mathbf{y}[f] = \mathbf{Q}_\nu \mathbf{r}[f], \quad (44)$$

where $\mathbf{r}[f] = \sum_{i=0}^{T-1} e^{-j2\pi fi/T} \mathbf{r}[i]$ and $\mathbf{y}[f] = \sum_{i=0}^{T-1} e^{-j2\pi fi/T} \mathbf{y}[i]$ are the Fourier transforms of the unprocessed signal vector and the received signal vector, respectively.

Selecting the equalizer scheme has been the subject of study in MIMO channel as in [9]. Two well-known equalizers are considered in this work:

- Zero-Forcing Equalizer (ZFE): As it was introduced earlier as a precoder, ZFE can bring down the ISI to zero. This equalizer is given by the following

$$\mathbf{Q}_\nu^{ZFE} = a_Q^{ZFE} (\mathbf{G}_\nu \mathbf{G}_\nu^H)^{-1} \mathbf{G}_\nu, \quad (45)$$

where a_Q^{ZFE} is the normalization factor, $\mathbf{G}_\nu = \sum_{l=0}^{L-1} e^{-j2\pi \nu l/L} \mathbf{G}_l$ is the Fourier transform of the composite channel matrix, and $\mathbf{G}_l = \hat{\mathbf{H}}_l^H$.

- Minimum Mean Square Error Equalizer (MMSEE): As it is known in the downlink channel as RZFP, MMSEE is able to maximize the power of received signal compared to the noise and interference. This equalizer can be obtained as

$$\mathbf{Q}_\nu^{MMSEE} = a_Q^{MMSEE} (\mathbf{G}_\nu \mathbf{G}_\nu^H + \beta_Q \mathbf{I}_K)^{-1} \mathbf{G}_\nu, \quad (46)$$

where a_Q^{MMSEE} is also a normalization factor and $\beta_Q \in \mathbb{R}^+$ is a system parameter just like the one in RZFP, which depends on the SNRs and the path losses of the users. By inspecting the similarities in the definition of MMSEE and RZFP, it can be concluded that MMSEE in the uplink performs the same functionality as RZFP in the downlink.

Considering the inverse Fourier transform of the equalizer matrix $\mathbf{Q}_m = \sum_{\nu=0}^{N-1} e^{j2\pi \nu m/N} \mathbf{Q}_\nu$, (44) can

be rewritten in the time domain as

$$\mathbf{y}[i] = \sqrt{\rho_f} \sum_{m=0}^{N-1} \sum_{l=0}^{L-1} \mathbf{Q}_m \hat{\mathbf{H}}_l \mathbf{s}[(i-l-m) \bmod T] + \sum_{m=0}^{N-1} \mathbf{Q}_m \mathbf{n}[i-m]. \quad (47)$$

Note that using an equalizer in the channel, the super channel state information matrix can be obtained by $\mathbf{F}_{(m,l)} = \mathbf{Q}_m \hat{\mathbf{H}}_l$. Similar to the downlink channel, one can rewrite the vector of the received signal using the desired signal and the effective noise terms

$$y_k[i] = g_k[i] + n'_k[i], \quad (48)$$

where $g_k[i]$ is the desired signal at the k -th user and time i

$$g_k[i] = \sqrt{\rho_f} \sum_{l=0}^{L-1} \mathbf{F}_{(-l,l)}[k, k] s_k[i]. \quad (49)$$

Note that the channel length is smaller than the frequency range (i.e., $N > L$). One can obtain the effective noise of the channel at the k -th user as the following

$$\begin{aligned} n'_k[i] = & \sqrt{\rho_f} \sum_{\substack{b=1-N \\ b \neq 0}}^{L-1} \sum_{l=L_1}^{L_3} \mathbf{F}_{(b-l,l)}[k, k] s_k[i-b] \\ & + \sqrt{\rho_f} \sum_{\substack{q=1 \\ q \neq k}}^K \sum_{b=1-N}^{L-1} \sum_{l=L_1}^{L_3} \mathbf{F}_{(b-l,l)}[k, q] s_q[i-b] + \sum_{q=1}^K \sum_{m=0}^{N-1} \mathbf{Q}_m[k] n_q[i-m], \end{aligned} \quad (50)$$

where it consists of ISI, MUI, and independent noise terms, respectively, missing the IF term that exists in the downlink channel.

C. Importance of Full Channel State Information at the Base Station

Note that, since this is uplink transmission, the full Channel State Information (CSI) is available at the base station. This enables expression of the desired response $g_k[i]$ as in (37) in the case of CFME and as (49) in the case of MMSEE and ZFE. If the full CSI were not available, for example, as it would be in the case of downlink transmission, $g_k[i]$ for CMFE would have to be expressed as

$$g_k[i] = \sqrt{\frac{\rho_f}{MK}} \left(\sum_{l=0}^{L-1} \mathbb{E}\{\mathbf{F}_{(l,l)}[k, k]\} \right) s_k[i \bmod T], \quad (51)$$

instead of (36), resulting in an additional interference term (IF)

$$\sqrt{\rho_f} \sum_{l=0}^{L-1} \left(\mathbf{F}_{(-l,l)}[k, k] - \mathbb{E}\{\mathbf{F}_{(-l,l)}[k, k]\} \right) s_k[i]. \quad (52)$$

in (38), and a similar condition would hold in the case of MMSEE and ZFE in (49) and (50), as was the case in (4) and (5). The IF interference represents the instantaneous wander of $\mathbf{F}_{(l,l)}[k, k]$ around its mean. In general, it causes a large degree of interference. Its absence in the uplink is a significant advantage.

IV. CORRELATION PATTERNS

In this section, two of the most well-known correlation patterns, the exponential correlation pattern and the Bessel function correlation pattern, are introduced and elaborated on. Considering the structure of the two patterns, the correlation matrix \mathbf{A} will remain symmetric.

A. Exponential Correlation Model

We will consider a linear antenna array for this correlation model. Assume antenna m_i is in position i and antenna m_j is in position j . It is reasonable to expect, and is evidenced in the literature, that the effect of these antennas on one another should be related to $|i - j|$ considering the dependency of the channel to be among the antennas. A basic correlation factor $0 < a < 1$ is considered, which shows the effects of antennas with respect to $|i - j|$ on each other, where a is a real number. One can obtain a correlation matrix based on this model in which the elements are $[\mathbf{A}]_{i,j} = a^{|i-j|}$. The matrix in this model is known as the exponential correlation matrix. This model is commonly employed when spatial correlation is considered for MIMO or spatial diversity channels [12], [13]. The correlation coefficient increases as the separation between antennas decreases. An S-parameter-based formulation shows that when only two monopoles are considered, the coefficient varies from 0.8 to about 0.2 when the antenna separation is about 0.05 to 0.2 times the wavelength [14]. A measurement study shows that, depending on propagation conditions, spatial correlation can remain significantly higher than 0.9 for a wide range of antenna separation values [15]. A range of average a values from 0.4 to 0.7 for antenna separations at approximately 0.25 to 0.5 wavelength was reported in [16].

B. Bessel Correlation Model

Another correlation model in MIMO systems is introduced in [17]. We refer to this model as the Bessel function correlation model. The (i, j) -th element of the new correlation matrix can be obtained by

$$[\mathbf{A}]_{i,j} = \frac{I_0(\sqrt{\eta^2 - 4\pi^2 d_{i,j}^2} + j4\pi\eta \sin(\mu)d_{i,j})}{I_0(\eta)}, \quad (53)$$

where $0 < \eta < \infty$ controls the width of the angle-of-arrival (AOA), $\mu \in [-\pi, \pi)$ is the mean direction of the AOA, I_0 is the zero-order modified Bessel function, and $d_{i,j}$ is the distance between j -th and i -th antenna normalized with respect to the wavelength [17]. We consider a linear array for the antenna elements at the base station in this model as well. Therefore, we can denote the distance between i -th

and j -th antenna as

$$d_{i,j} = |i - j|d, \quad (54)$$

where d is the distance between adjacent antenna elements, normalized with respect to the wavelength.

In the model in (53), $\mu = 0$ corresponds to the perpendicular direction from the linear antenna array (broadside direction), while $\mu = \pm\pi/2$ correspond to the parallel direction to the linear antenna array (end-fire or inline direction). In this paper, we will study the broadside case of $\mu = 0$. Note that, when $\mu = 0$, since $I_0(x)$ is a uniformly increasing function of x , $[\mathbf{A}]_{i,i} = 1$, $[\mathbf{A}]_{i,j} < [\mathbf{A}]_{i,k}$ for $k > j$, and \mathbf{A} will be symmetric. Our focus with this model in this paper is on the spatial multiplexing of closely spaced users positioned in the same beam of the massive array. Other values of μ , together with spatial multiplexing of multiple users with different AOA, are left as future work.

V. COMPUTATION RESULTS

For the purpose of computations, PDP is considered to be exponential with $L = 4$ and $d_l[k] = \frac{e^{-\theta_k l}}{\sum_{i=0}^3 e^{-\theta_k i}}$, $l = \{0, \dots, 3\}$, where $\theta_k = \frac{K-1}{5}$, $k = \{1, \dots, K\}$ as in [1]. Note that the achievable sum-rate is invariant of the channel PDP. Hence, any other PDP which satisfies (2) can also be considered. Fig. 1 of [1] shows the achievable sum-rate of CMFP via theoretical analysis and computation in an i.i.d. channel. In this case, the two results perfectly match. The analysis in this paper reduces to that in [1] for $\mathbf{A} = \mathbf{I}$. On the other hand, Fig. 2 of [1] provides typical scenarios in an i.i.d. channel, where the minimum required transmit power to achieve a fixed information rate per each user is shown for CMFP and OFDM transmission.

Since the CMFP matrix is the Hermitian of the channel response, the process that is taken to normalize the precoder response matrix does not affect the power of the desired signal in the downlink, and therefore, the upper bound of the channel remains the same as the correlation parameter changes. The upper bound and achievable sum-rate of the system are given by (31) and (32), respectively. In Fig. 1 and Fig. 2 only one upper bound has been shown. For ZFP and RZFP on the other hand, the case is different. As the precoder response matrix does not match the channel response matrix and the process of normalizing the precoder response matrix is designed specifically for each precoder individually, the changes in the correlation parameter affect the normalization factors, and therefore, the power of the desired signal in the system, and eventually, the capacity of the channel (i.e., the upper bound). Hence, there are multiple upper bounds shown in Fig. 3 to Fig. 6. The argument for CMFP and the downlink channel holds for CMFE and the uplink channel. Thus, the cases for ZFE and MMSEE are the same as those of ZFP and

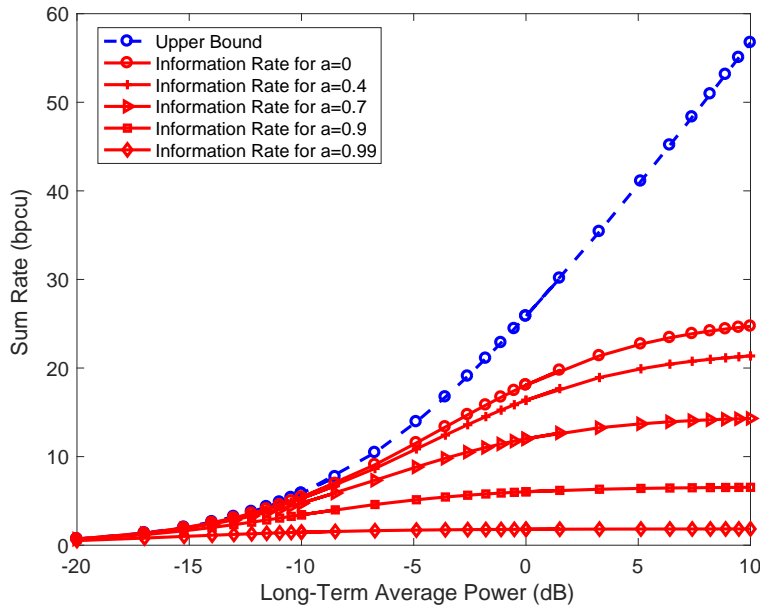


Fig. 1. Comparison between the achievable rate of CMFP in a downlink channel under the exponential correlation pattern with different correlation parameter $a \in \{0, 0.4, 0.7, 0.9, 0.99\}$. Note that based on the formulation for SNR in the channel, normalization is the same for all values of the correlation parameter. Therefore, only one upper bound is shown for all values of a . Also note that the number of antennas at the base station is $M = 50$, the number of users is $K = 10$, the number of taps used in the computations is $L = 4$, and the block length in the time domain is $T = 100$.

RZFP. The reason for this is the fact that their responses do not match the channel response either. That is the reason multiple upper bounds are shown in the Fig. 12 to Fig. 15.

In Fig. 1 the performance of CMFP in the downlink channel is shown and compared under the influence of the exponential correlation pattern with the correlation parameter a . It can be seen that by increasing the correlation parameter a , the information rate of CMFP decreases dramatically. This figure implies that CMFP may not be a good candidate in a correlated channel with a large correlation parameter, since there is a huge gap between the information rate for $a \in \{0.9, 0.99\}$ and the upper bound capacity of the channel. Note that the gap is still substantial for $a = 0.7$. Based on the computation results, one can say that the loss in the achievable rate is negligible as long as the correlation parameter is less than 0.5 as it is also stated in [18].

As specified earlier, in this paper μ is taken as 0 in the computations. The parameter η decreases the achievable rate of the system dramatically by changing from 0 (isotropic scattering) to ∞ (extremely non-isotropic). The isotropic scattering model, also known as the Clarke's model, corresponds to the uniform distribution for the angle of arrival (AOA). However, empirical measurements have shown that the AOA distribution of waves impinging on the user is more likely to be nonuniform [17]. It is shown in [19] that values of η show a very large variation, pointing out to the substantial change in the achievable rate with this fact of propagation.

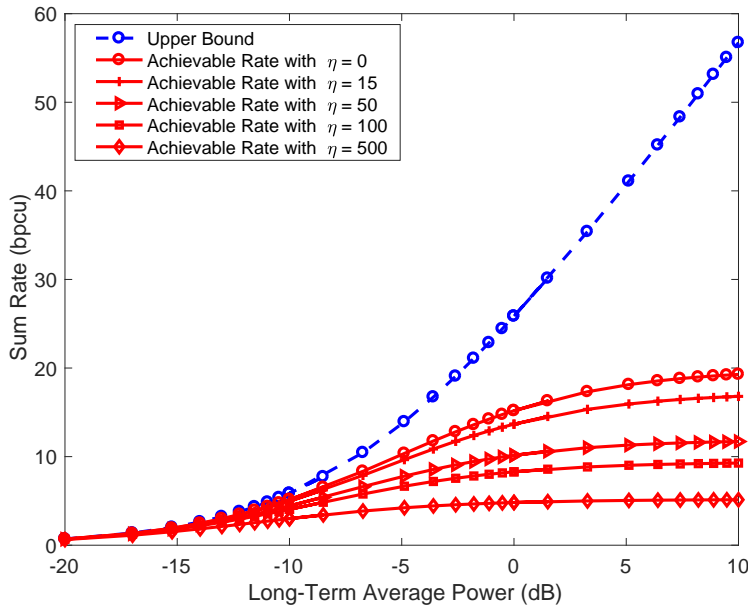


Fig. 2. The effect of the parameter $\eta \in \{0, 15, 50, 100, 500\}$ on the achievable rate for CMFP in a channel with Bessel correlation model. The mean direction of AOA is 0 and the distance between adjacent antenna elements is considered to be $d = 0.5$. System parameters are $M = 50$, $K = 10$, $L = 4$, $T = 100$.

The performance of CMFP that is shown in Fig. 2 is affected by the Bessel correlation pattern where the influence of the parameter η has been studied. The mean direction of AOA is considered to be 0 and the distance between adjacent antenna element in the model is set to be 0.5 normalized with respect to the wavelength. It can be seen that the starting point (i.e., when $\eta = 0$) of the achievable rate in the channel under the influence of the Bessel correlation pattern is lower than the starting point (i.e., when $a = 0$) of the one under the influence of the exponential correlation pattern. As the correlation parameter η grows, one can see that the achievable rate for the users in the channel decreases, the same behavior in the channel under the influence of the exponential correlation pattern, which shows the incapability of CMFP to be considered for a highly correlated channel.

One can see the performances of the conventional precoders (introduced in Section II) on the downlink channel under the exponential correlation pattern in Fig. 3 and Fig. 4. In order to run the computations for RZFP, we set the value for the system parameter β_W in the manner to maximize the sum-rate of the users. How to find such optimal β_W is described in [2], [20]. In each figure, a comparison is made to show how the information rate changes as the correlation parameter a increases for different precoders in the downlink channel. Note that in these figures, due to the dependency of the normalization factor on the correlation parameter, upper bound curves change as the correlation parameter changes.

A comparison between Fig. 1 and Fig. 3 shows that for correlation parameter larger than $a = 0.7$, ZFP shows slightly better achievable rate. Due to the higher sensitivity of CMFP to the correlation parameter,

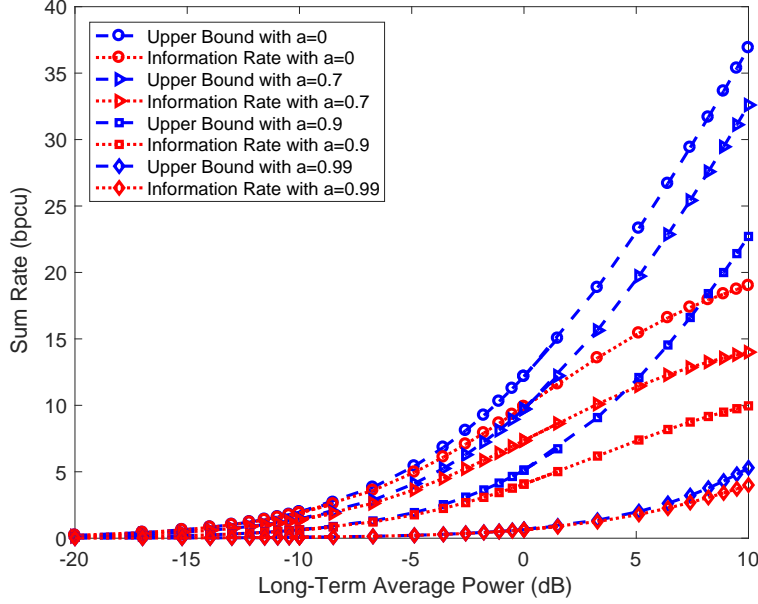


Fig. 3. Capacity and information rate for ZFP in a downlink channel under the exponential correlation pattern with correlation parameter $a \in \{0, 0.7, 0.9, 0.99\}$. System parameters are $M = 50$, $K = 10$, $L = 4$, and $T = 100$. In addition, the block length in the frequency domain is $N = 20$.

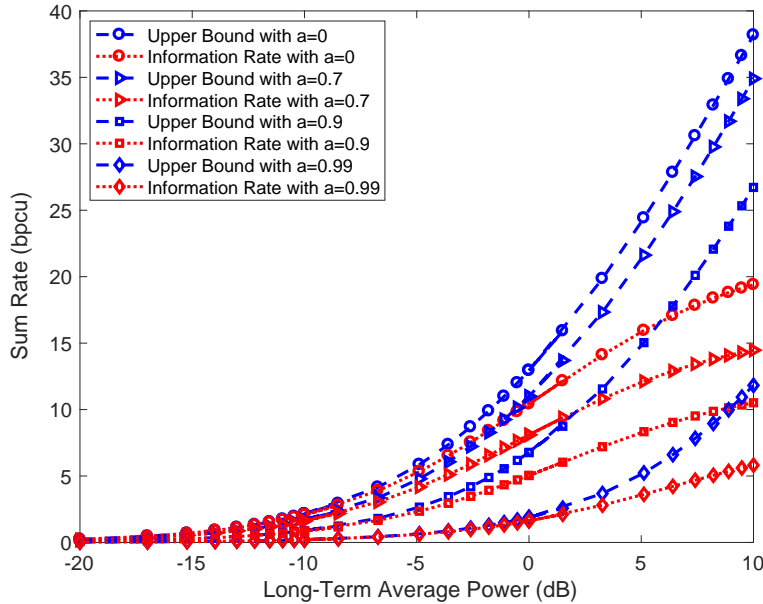


Fig. 4. Upper bound and achievable rate of a downlink channel under the exponential correlation pattern with correlation parameter $a \in \{0, 0.7, 0.9, 0.99\}$ using RZFP. System parameters are $M = 50$, $K = 10$, $L = 4$, $T = 100$, and $N = 20$.

one can conclude that ZFP has superiority in highly-correlated channels. Also, it can be seen that the ZFP and RZFP perform equally well when the number of users is small [2]. Considering the fact that RZFP has an optimal valued parameter (i.e., β) and because of its ability to balance the resulting array gain and the amount of inter-user interference received by the users, RZFP has an advantage over ZFP when it comes to a larger number of users [2].

Fig. 5 and Fig. 6 show the performance of the two introduced conventional precoders in a downlink

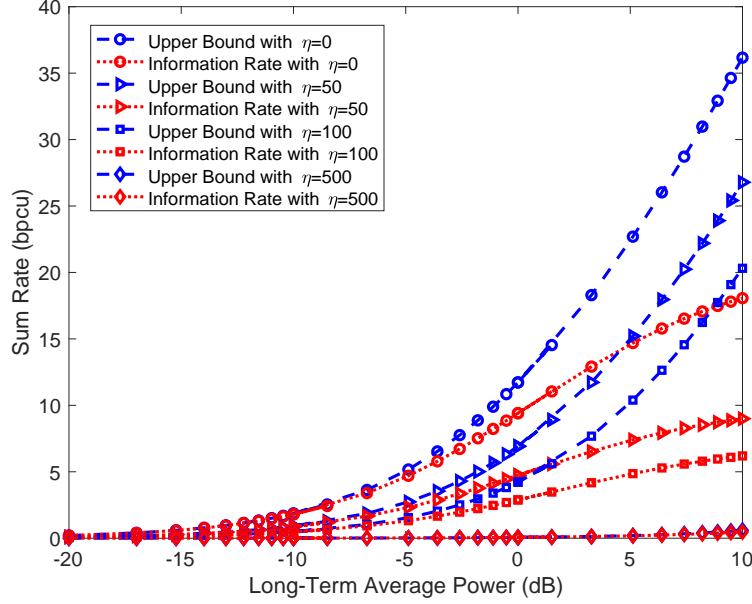


Fig. 5. Capacity and information rate for ZFP in a channel under the Bessel correlation pattern with correlation parameter $\eta \in \{0, 50, 100, 500\}$. Note that the mean direction of AOA is set to be 0 and the distance between adjacent antenna elements is $d = 0.5$. System parameters are $M = 50$, $K = 10$, $L = 4$, $T = 100$, $N = 20$.

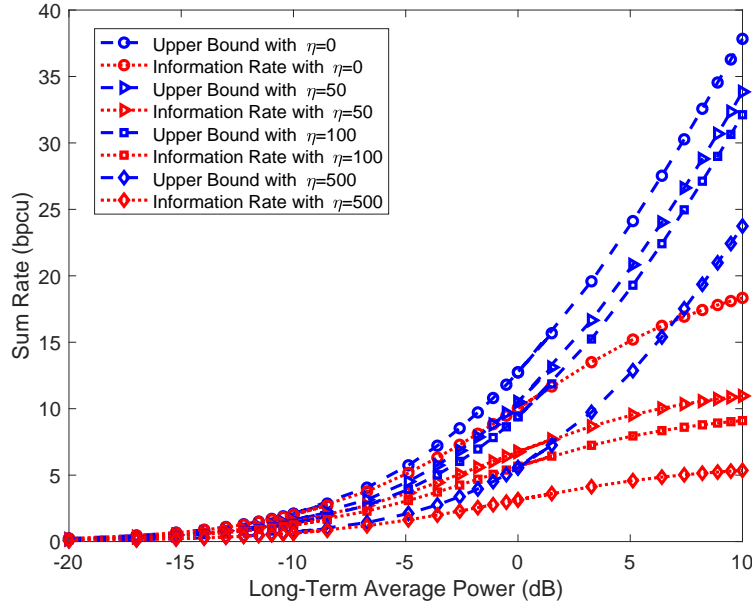


Fig. 6. Upper bound and achievable rate of a channel with Bessel model parameter $\eta \in \{0, 50, 100, 500\}$ using RZFP. In the same situation, the mean direction of AOA is 0 and the distance between adjacent antenna elements is $d = 0.5$. System parameters are $M = 50$, $K = 10$, $L = 4$, $T = 100$, $N = 20$.

channel affected by the Bessel correlation pattern with the variable parameter η . Again, note that in these computations, β_W is chosen in an optimal manner. Each figure shows how the parameter η changes the achievable rate of the precoders. One can see that when $\eta \geq 100$, both precoders outperform CMFP. In these figures, upper bound curves change due to the dependency of the normalization factor on the correlation parameter.

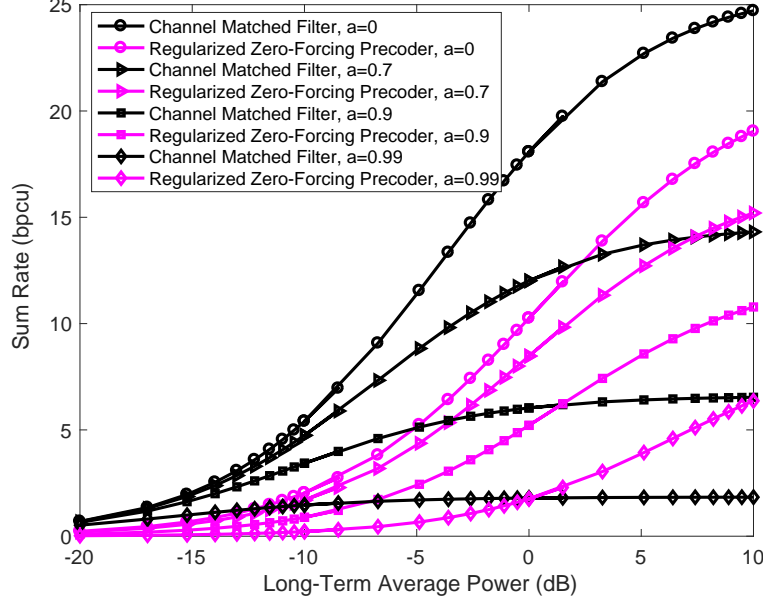


Fig. 7. Performance of CMFP and RZFP in terms of achievable rate in a downlink channel under the exponential correlation pattern with different correlation parameters $a \in \{0, 0.7, 0.9, 0.99\}$. System parameters are $M = 50$, $K = 10$, $L = 4$, $T = 100$, $N = 20$.

Fig. 7 shows a comparison between RZFP and CMFP in terms of the information rate in a downlink channel with the exponential correlation pattern. When the channel is correlation-free ($a = 0$), it is the CMFP that shows better performance and higher achievable data rate and, as SNR increases, the gap between the information rates of the two increases. However, by increasing the correlation parameter in the channel, RZFP shows its superiority in providing higher information rate in the channel. This behavior was discussed in [9] as a general possibility.

Further investigation shows the same comparison when the number of users increase to $K = 15$ and the range of transmitted power increases to 40 dB, respectively. The information rate of RZFP for higher SNRs passes that of CMFP, even in an i.i.d. channel. In addition, saturation occurs faster and sooner for CMFP.

In Fig. 8, CMFP and RZFP are compared in a downlink channel with the Bessel correlation pattern. One can see that the effect of the parameter η on RZFP is stronger than that of the exponential correlation pattern. However, when $\eta \geq 500$, RZFP shows a better result compared to CMFP.

Fig. 9 shows the performance of CMFP and RZFP under the Bessel correlation model, where the distance between adjacent antenna elements in a linear antenna model is considered to be $d = \{0.125, 0.25, 0.5\}$, normalized with respect to the wavelength. Note that, unlike as in the exponential correlation model, CMFP performs better than conventional precoders (RZFP performance is shown in Fig. 8) in the SNR range of $[-20 \text{ dB}, 15 \text{ dB}]$ (except for $d = 0.125$). For SNRs higher than 15 dB, RZFP has superior

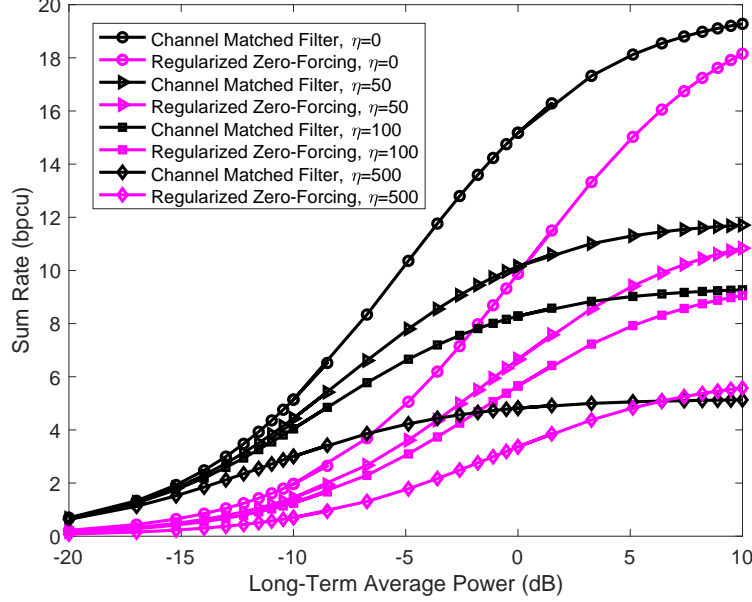


Fig. 8. A comparison between performance of CMFP and RZFP in a downlink channel under the Bessel correlation pattern with different correlation parameters $\eta \in \{0, 50, 100, 500\}$. System parameters are $M = 50$, $K = 10$, $L = 4$, $T = 100$, $N = 20$.

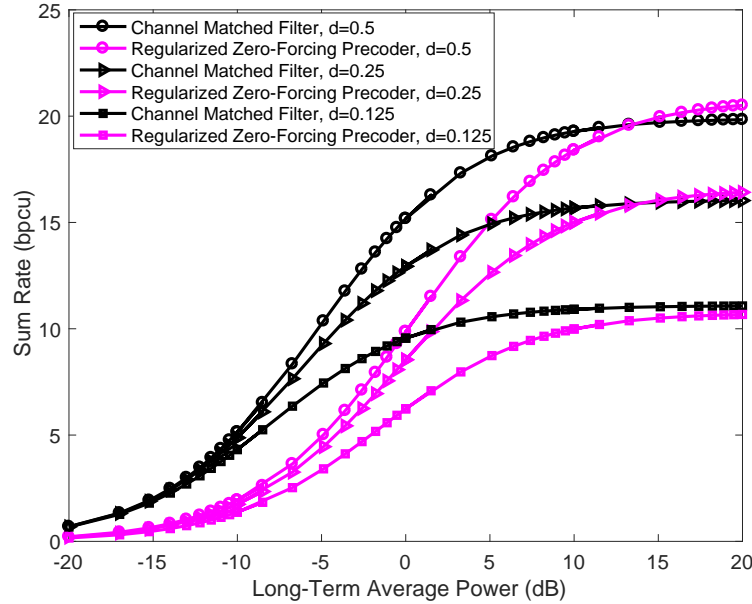


Fig. 9. Performance of CMFP and RZFP in a channel with Bessel correlation model and three different distances between adjacent antenna elements in a linear format $d \in \{0.125, 0.25, 0.5\}$. Note that AOA is set to be 0. System parameters are $M = 50$, $K = 10$, $L = 4$, $T = 100$, $N = 20$.

performance (except in the case that $d = 0.125$ for which it occurs at higher SNR).

It is also noteworthy to mention that observations of the computations showed that employment of the precoders in the time domain rather than frequency domain in the downlink channel improves the achievable rate of the system in the low-SNR regions while saturating faster in the higher SNRs. Precoders in the frequency domain on the other hand, showed better performance in terms of achievable rate in the downlink channel when SNR grows. They also showed less sensitivity to the correlation pattern in the

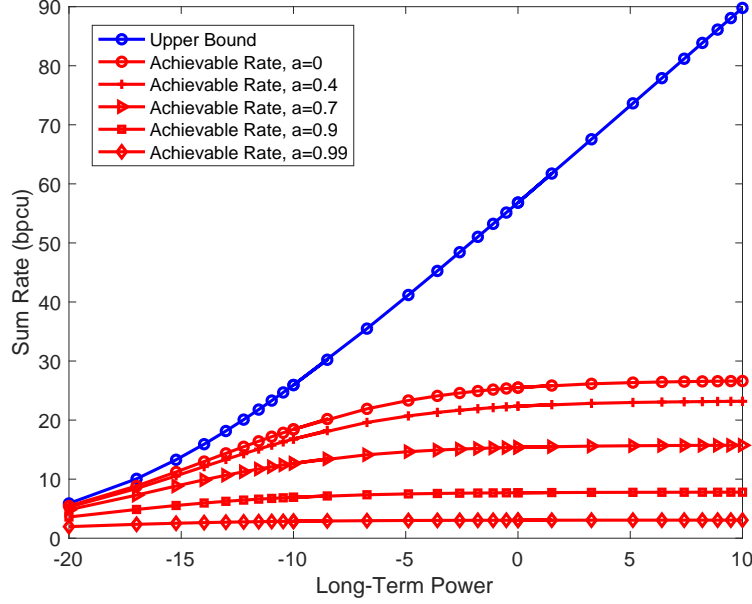


Fig. 10. CMFE performance in terms of achievable rate in the uplink channel under the influence of the exponential correlation pattern, the correlation parameter changes as $a \in \{0, 0.4, 0.7, 0.9, 0.99\}$. System parameters are $M = 50$, $K = 10$, $L = 4$, $T = 100$, $N = 20$, $T_c = 20$.

channel, meaning that in a correlated channel, using the precoders in the frequency domain makes more sense.

In Fig. 10 and Fig. 11, the performance of CMFE in the uplink channel is shown and compared under the influence of the exponential and the Bessel correlation pattern, respectively. It can be seen that by increasing the correlation parameter (i.e., either a or η), the information rate of CMFE decreases dramatically. This fact shows that CMFE may not be a good candidate in a correlated channel with a large correlation parameter, since there is a huge gap between the information rate and the upper bound capacity as we increase the correlation parameter. Note that in Fig. 11, the mean direction of AOA is considered to be 0 and the distance between adjacent antenna element in the model is set to be 0.5 normalized with respect to the wavelength. It can be seen that the starting point (i.e., when $\eta = 0$) of the achievable rate in the channel under the influence of the Bessel correlation pattern is lower than the starting point (i.e., when $a = 0$) of the one under the influence of the exponential correlation pattern.

Fig. 12 and Fig. 13 show the performance of ZFE and MMSEE, respectively, under the exponential correlation pattern. In order to obtain β_Q to run the computations for MMSEE, we used the same procedure to obtain β_W for RZFP, in the way to maximize the users' sum-rate with respect to the received SNR, see, i.e., [2] and [20]. The results of the computations in these figures show that not only MMSEE shows a higher upper bound, but also it shows a better achievable rate and less sensitivity to the exponential correlation parameter. Fig. 14 and Fig. 15 show the same criteria for the equalizers under the Bessel

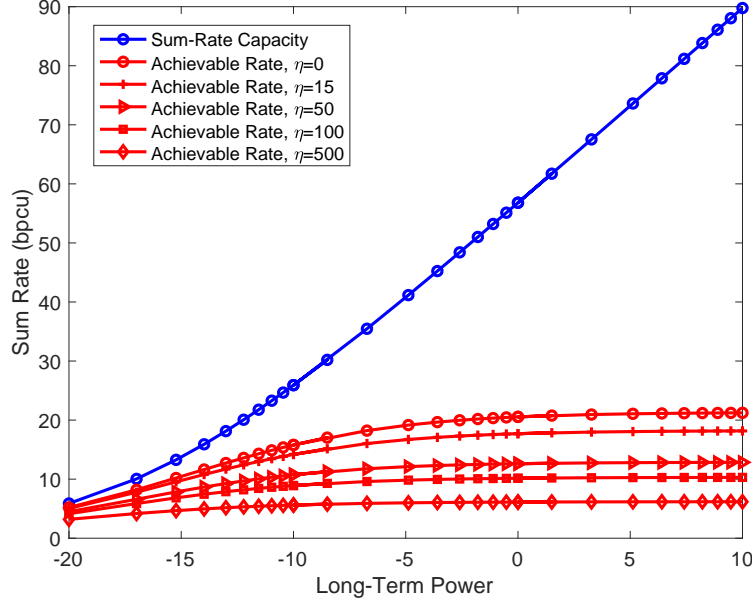


Fig. 11. Achievable rate of the uplink channel using CMFE under the influence of the Bessel correlation pattern is considered with the correlation parameter $\eta \in \{0, 15, 50, 100, 500\}$. System parameters are $M = 50$, $K = 10$, $L = 4$, $T = 100$, $N = 20$, $T_c = 20$.

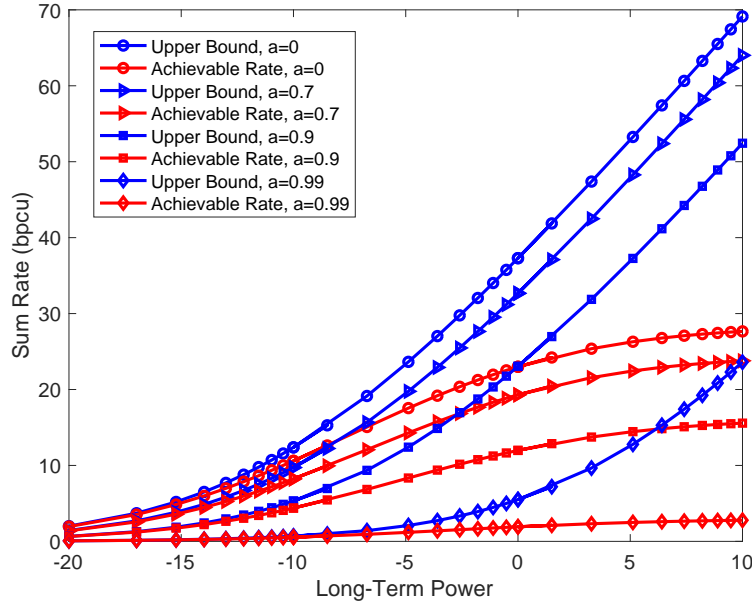


Fig. 12. Achievable rate of the uplink channel using ZFE, the exponential correlation pattern is considered with the correlation parameter $a \in \{0, 0.7, 0.9, 0.99\}$. System parameters are $M = 50$, $K = 10$, $L = 4$, $T = 100$, $N = 20$, $T_c = 20$.

correlation pattern. A better achievable rate, higher upper bound, and less sensitivity to the correlation pattern can also be observed in these figures. Comparing Fig. 13 and Fig. 15 makes it clear that MMSEE shows less sensitivity to the parameter η of the Bessel correlation pattern rather than the parameter a of the exponential pattern.

Comparing the frequency- and time-domain equalizers and observing the computations, equalizers which were employed in the frequency domain showed a better performance in the low-SNR regions as well

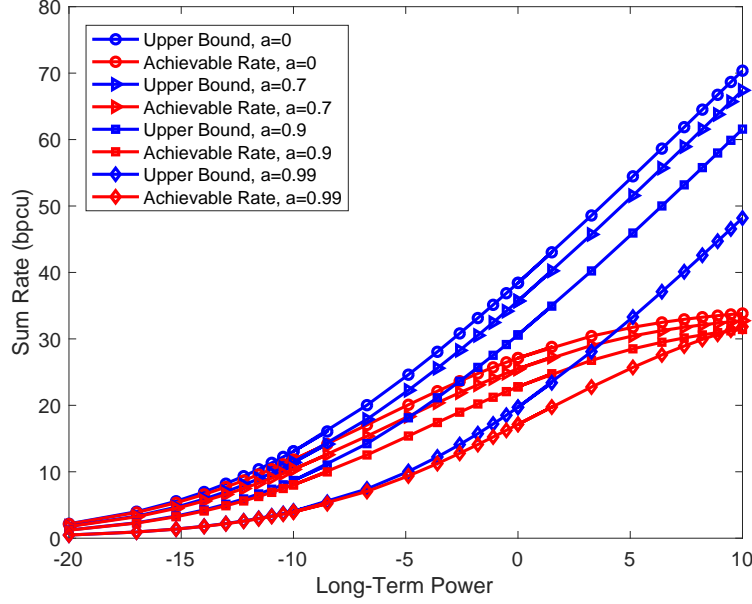


Fig. 13. Performance of MMSEE in the uplink channel with the exponential correlation pattern with the correlation parameter $a \in \{0, 0.7, 0.9, 0.99\}$. System parameters are $M = 50$, $K = 10$, $L = 4$, $T = 100$, $N = 20$, $T_c = 20$.

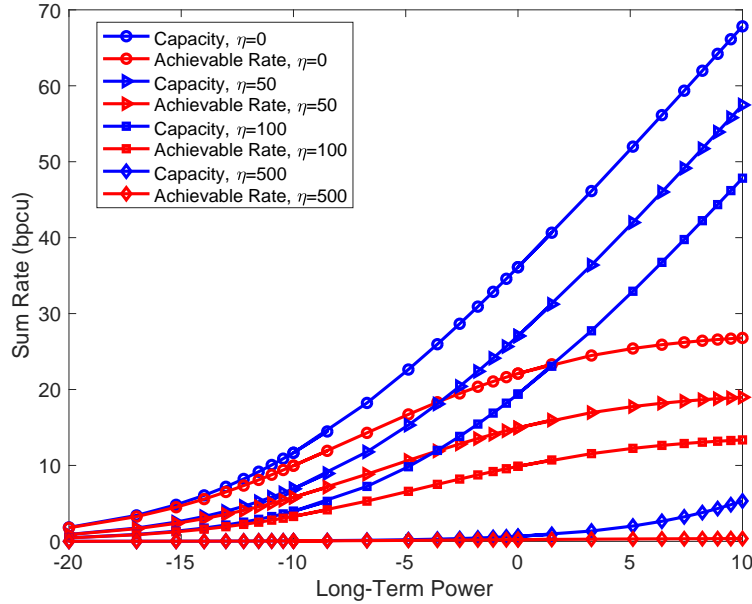


Fig. 14. Bit rate of the users in the uplink channel when ZFE is used in a channel with the Bessel correlation pattern. The distance between adjacent antenna elements is set to be $d = 0.5$ normalized with respect to the wavelength and AOA is set to be 0. System parameters are $M = 50$, $K = 10$, $L = 4$, $T = 100$, $N = 20$, $T_c = 20$.

as high-SNR ones. Also, less sensitivity to the correlation patterns was observed. In addition to this, the employment of the equalizers in the frequency domain is computationally simpler than employment of them in the time domain and essentially, the performance of the frequency-domain equalizers in the single-carrier modulation is the same as that of a system using OFDM technique [8].

A study of the achievable rates is provided in Fig 16 for the correlated channel with $a = \{0.7, 0.9, 0.99\}$. In these comparative figures, one can observe that the performance of both MMSEE as well as ZFE

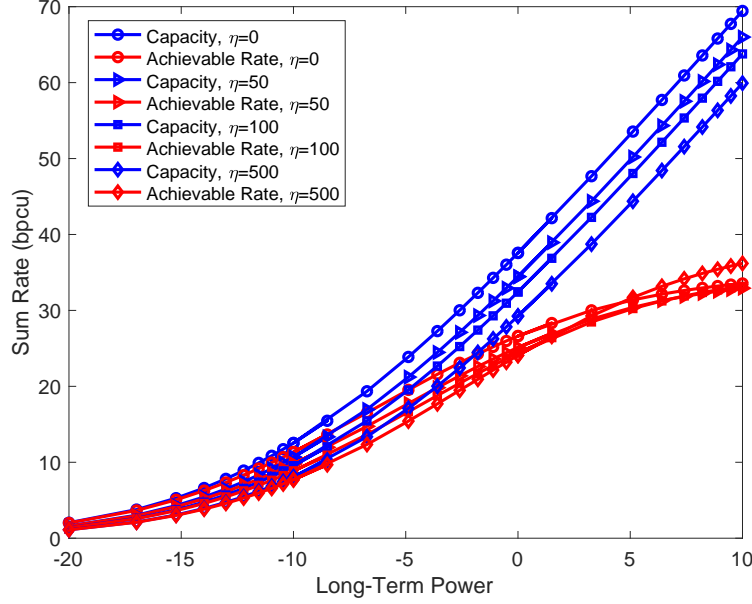


Fig. 15. Performance of MMSEE in the uplink channel with the Bessel correlation pattern, the distance between adjacent antenna elements is $d = 0.5$ and AOA is set to be 0. System parameters are $M = 50$, $K = 10$, $L = 4$, $T = 100$, $N = 20$, $T_c = 20$.

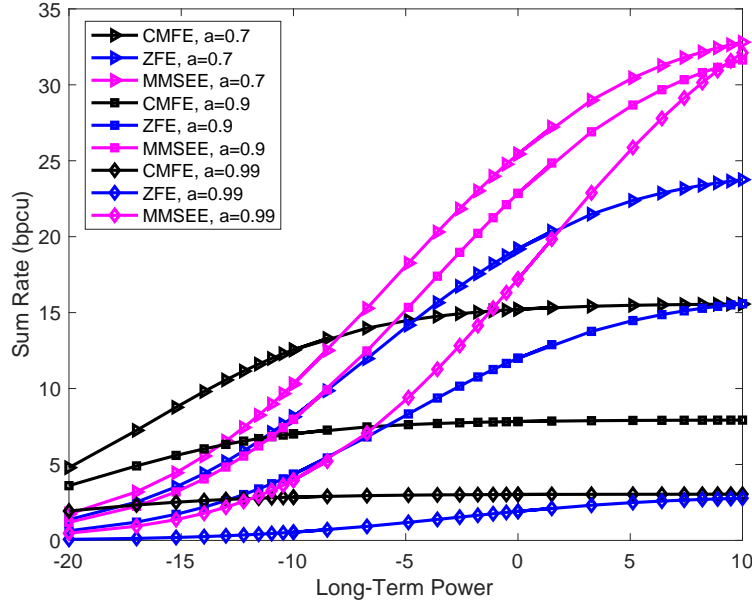


Fig. 16. Achievable rates for CMFE, MMSEE, and ZFE in an uplink channel with $a = 0.7, 0.9$, and 0.99 .

improve against CMFE. MMSEE performance is improved very significantly, even in the case of high correlation, such as $a = 0.9$ and $a = 0.99$. It is worthwhile to observe that there exists a gain for ZFE as well. With this gain, ZFE can outperform CMFE. Since the design of ZFE is simpler in that it does not require the parameter β_W , this is an important observation.

VI. CONCLUSION

As a result of the analysis and computations in this work, one can say that the sum-rate of a channel is highly dependent on the nature of the channel. For uncorrelated downlink channels, CMFP has optimal performance and it does perform near the upper bound of the channel. However, the presence of correlation among the antennas at the base station leads to a decrease in the achievable sum-rate for the users in the system. Depending on the correlation model and the channel SNR, it is possible to employ another precoder to improve the sum-rate performance. In particular, RZFP can outperform the matched-filter precoder as far as the downlink channel is concerned.

Looking at the uplink results, one might conclude that using MMSEE (which is equivalent of RZFP) can improve the data-rate in the channel. Using the Channel Matched Filter technique in the uplink as an equalizer leads to a better performance of the system, higher bit-rate for the users, and higher sum-capacity in the channel. As it is shown for MMSEE, it is less sensitive to the correlation patterns considered in this paper and can be a good choice to use in the system when channel with high correlations are concerned.

Employment of precoders in the downlink channel and equalizers in the uplink channel is needed because of implementation and Channel State Information (CSI) considerations. In both cases, the precoder or the equalizer is placed at the base station. Trying to implement the same functionality at the user terminals would not be practical due to CSI considerations.

APPENDIX

Let $\mathbf{F}_{(l,l-b)}[k, q] \triangleq d_l^{1/2}[k] \mathbf{h}_l[k] \mathbf{A} \mathbf{h}_{l-b}[q] d_{l-b}^{1/2}[q]$ and $T \triangleq T_{l,l',b}[k, q] \triangleq \mathbb{E}\{(\mathbf{F}_{(l,l-b)}[k, q])(\mathbf{F}_{(l',l'-b)}[k, q])^*\}$.

Then,

$$k = q, l = l', b = 0 \Rightarrow T = (\text{tr}(\mathbf{A}^2) + \text{tr}^2(\mathbf{A}))d_l^2[k], \quad (55)$$

$$k = q, l = l', b \neq 0 \Rightarrow T = \text{tr}(\mathbf{A}^2)d_l[k]d_{l-b}[k], \quad (56)$$

$$k = q, l \neq l', b = 0 \Rightarrow T = \text{tr}^2(\mathbf{A})d_l[k]d_{l'}[k], \quad (57)$$

$$k = q, l \neq l', b \neq 0 \Rightarrow T = 0, \quad (58)$$

$$k \neq q, l = l', b = 0 \Rightarrow T = \text{tr}(\mathbf{A}^2)d_l[k]d_l[q], \quad (59)$$

$$k \neq q, l = l', b \neq 0 \Rightarrow T = \text{tr}(\mathbf{A}^2)d_l[k]d_{l-b}[q], \quad (60)$$

$$k \neq q, l \neq l' \Rightarrow T = 0. \quad (61)$$

REFERENCES

- [1] A. Pitarokoilis, S. K. Mohammed, and E. G. Larsson, "On the optimality of single-carrier transmission in large-scale antenna systems," *IEEE Wireless Commun. Lett.*, vol. 1, pp. 276–279, Aug 2012.
- [2] C. Mellon, E. G. Larsson, and T. Eriksson, "Waveforms for the massive MIMO downlink: Amplifier efficiency, distortion and performance," *IEEE Trans. Commun.*, vol. 64, pp. 5050–5063, Dec 2016.
- [3] F. Rusek, D. Perrsson, B. K. Lau, E. G. Larsson, T. L. Marzetta, O. Edfors, and F. Tufvesson, "Scaling up MIMO: Opportunities and challenges with very large arrays," *IEEE Signal Process. Mag.*, vol. 30, pp. 40–60, Jan 2013.
- [4] E. G. Larsson, O. Edfors, F. Tufvesson, and T. L. Marzetta, "Massive MIMO for next generation wireless systems," *IEEE Commun. Mag.*, vol. 52, pp. 186–195, Feb 2014.
- [5] A. Pitarokoilis, S. K. Mohammed, and E. G. Larsson, "Achievable rates of ZF receivers in massive MIMO with phase noise impairments," in *Proc. Asilomar Conf. Signals, Sys. Comput.*, Nov 2013, pp. 1004–1008.
- [6] S. Ajey, B. Srivalli, and G. V. Rangaraj, "On performance of MIMO-OFDM based LTE systems," *Conf. Wireless Commun. and Sensor Comput.*, pp. 1–5, Jan 2010.
- [7] E. Ayanoglu, V. K. Jones, G. G. Raleigh, J. Gardner, D. Gerlach, and K. Toussi, "VOFDM broadband wireless transmission and its advantages over single-carrier modulation," in *IEEE Int. Conf. Commun.*, Jun 2001, pp. 1660–1664.
- [8] D. Falconer, S. L. Ariyavisitakul, A. Benyamin-Seeyar, and B. Eidson, "Frequency domain equalization for single-carrier broadband wireless systems," *IEEE Commun. Mag.*, vol. 40, pp. 58–66, Apr 2002.
- [9] A. H. Mehana and A. Nosratinia, "Diversity of MIMO linear precoding," *IEEE Trans. Inf. Theory*, vol. 60, pp. 1019–1038, Feb 2014.
- [10] P. Yang, Y. Xiao, Y. L. Guan, K. V. S. Hari, A. Chockalingam, S. Sugiura, H. Haas, M. D. Renzo, C. Masouros, Z. Liu, L. Xiao, S. Li, and L. Hanzo, "Single-carrier SM-MIMO: A promising design for broadband large-scale antenna systems," *IEEE Commun. Surveys & Tutorials*, vol. 18, pp. 1687–1716, Feb 2016.
- [11] N. Beigiparast, G. M. Guvensen, and E. Ayanoglu, "The effect of antenna correlation in single-carrier massive MIMO transmission," in *IEEE 87th Vehicular Technology Conference – Spring*, Jun. 2018, pp. 1–7.
- [12] V. A. Aalo, "Performance of maximal-ratio diversity systems in a correlated Nakagami-fading environment," *IEEE Trans. Commun.*, vol. 43, pp. 2360–2369, Aug 1995.
- [13] E. Bjornson, E. Jorswieck, and B. Ottersten, "Impact of spatial correlation and precoding design in OSTBC MIMO systems," *IEEE Trans. Inf. Theory*, vol. 9, pp. 3578–3589, Nov 2011.
- [14] X. Wang, H. D. Nguyen, and H. T. Hui, "Correlation coefficient expression by S-parameters for two omni-directional MIMO antennas," in *IEEE Int. Symp. Antennas Propag. (APSURSI), Spokane, WA, 2011*, Jul 2011, pp. 301–304.
- [15] A. Intarapanich, P. L. Kafle, R. Davies, A. Sesay, and J. McRory, "Spatial correlation measurements for broadband MIMO wireless channels," in *Proc. IEEE 60th Vehicular Technology Conference, (VTC2004-Fall)*, vol. 1, Sept 2004, pp. 52–56.
- [16] M. K. Samimi, S. Sun, and T. S. Rappaport, "MIMO channel modeling and capacity analysis for 5G millimeter-wave wireless systems," in *10th European Conference on Antennas and Propagation (EuCAP)*, Apr 2016.
- [17] A. Abdi and M. Kaveh, "A space-time correlation model for multielement antenna systems in mobile fading channels," *IEEE J. Sel. Areas Commun.*, vol. 20, pp. 550–560, Apr 2002.
- [18] M. Chiani, M. Z. Win, and A. Zanella, "On the capacity of spatially correlated MIMO Rayleigh-fading channels," *IEEE Trans. Inf. Theory*, vol. 49, pp. 2363–2371, Oct 2003.
- [19] A. Abdi, J. A. Barger, and M. Kaveh, "A parametric model for the distribution of the angle of arrival and the associated correlation function and power spectrum at the mobile station," *IEEE Transactions on Vehicular Technology*, vol. 51, pp. 425–434, May 2002.

- [20] L. You, X. Gao, X. G. Xia, N. Ma, and Y. Peng, "Pilot reuse for massive MIMO transmission over spatially correlated Rayleigh fading channels," *IEEE Trans. Wireless Commun.*, vol. 14, pp. 3352–3366, Jan 2015.